



---

## MODELING OF METAL REMOVAL RATE BASED ON THE MECHANICS OF MATERIAL REMOVAL IN ULTRASONIC MACHINING

Abhinesh Bhaskar<sup>1</sup> and Jitendra kumar<sup>2</sup>

<sup>1</sup>Department of Mechanical, Government Engineering College, Banda  
, Banda, Uttar Pradesh, INDIA 210001

E-mail address: [abhineshjsss@gmail.com](mailto:abhineshjsss@gmail.com)

<sup>2</sup>Department of Mechanical, Government Engineering College, Banda  
, Banda, Uttar Pradesh, INDIA 210001

---

### **ABSTRACT:**

USM is unconventional machining process. Performance of any machining process is evaluated in terms of machining rate. Higher machining rate are desirable for better performance of any machining process. Comprehensive qualitative and quantitative analysis of the material removal mechanism and subsequently the development of analytical models of material removal are necessary for a better understanding and to achieve the optimum process performance. Analytical Material Removal models are also necessary for simulation, optimization and planning (i.e. operation and process planning) of the process, prediction of process performance indicators, verification and improvements of experimental results, selection of appropriate models for specific type of work material and machining conditions, etc. Since various investigators have proposed different analytical models of material removal as functions of controllable process variables. A continual need for a comprehensive and exhaustive review of various analytical material removal models for ultrasonic machining processes is being felt. This work is intended to fulfill this need in the area of ultrasonic machining. Various analytical and some semi-empirical/empirical material removal models for ultrasonic machining processes have been comprehensively and exhaustively reviewed, and have presented a material removal process incorporating the concepts of elasticity of work piece and tool in ultrasonic machining to improve MRR and compare it with experimental results. In our model we graphically analyses MRR with various input variables such as static force, amplitude, grit size etc. & compare it with experimental results.

---

### **1 Introduction:**

The history of USM began with a patent granted to L. Balamuth [1] in 1945. Shaw MC [2] was the first researcher to propose a static and simple analytical model giving the relationship between MRR and vibration amplitude, frequency, abrasive grit size and concentration, and feed force assuming all abrasive are identical, solid, rigid, spherical in shape. But, its predictions do not agree well with experimental observations. G.E. Miller [3] developed an MRR model based on plastic deformation restricting its application to ductile materials only assuming

all abrasives are cubical in size. V.I.Dikushin and Barke[4] related the energy consumed in removing the material from the work to the amplitude and force of vibration based on the laws of conservation of energy and momentum. The theory, however, could not explain the physics of the USM process. Rosenberg and Kazantsev [5] included the statistical distribution of abrasive particle size in their computationally intensive model assuming abrasives particle are incompressible and irregular in shape. Its solution requires numerical integration. Cook NH [6] proposed the simplest static model to predict linear

machining rate assuming abrasive grains are spherical in shape with uniform radius. This model predicts linear relationships between static stress and MRR, while MRR drops after a certain value of feed force. Kainth et al. [7] proposed another static and complicated model using the abrasive particle size distribution assuming abrasive particles are spherical in shape. The model does not predict a drop in machining rate after optimum value of grit size is reached. Nair and Ghosh [8] also proposed another computation intensive model simulating the principles of elastic wave propagation assuming abrasive particles are rigid spheres. Derivation of the model is computationally extensive. Pei et al. [9] works on a mechanistic approach to the prediction of MRR in rotary ultrasonic machining. Kamoun [10] set up a semi-elliptical model to predict MRR in stationary mode. They suggested that the material removal in ultrasonic contour machining is due to the propagation and fusion of lateral cracks which grow beneath the work surface. However, this model does not meet with experimental results. Wang and Rajurkar [11] suggested a more realistic model taking into account the stochastic and dynamic nature of the process assuming the work piece to be semi-infinite solid. But, this is applicable to perfectly brittle materials only. Lee T C and Chan C W [12] developed an analytical model to predict the effects of vibration amplitude, grit size and feed force on MRR and surface roughness for ceramic composites. Wiercigroch et al. [13] have proposed another model to predict the MRR in ultrasonic drilling using an impact oscillator approach. The inherent non-linearity of the discontinuous impact process has been modeled to generate the pattern of impact forces. This model explains the experimentally observed fall in MRR at higher static forces. Chaeng et al. [14] works on the machining characteristics of titanium alloy (Ti±6Al±4V) using a combination process of electro-discharge machining (EDM) with ultrasonic machining (USM). This combination EDM/USM process can increase the MRR and decrease the

thickness of the recast layer. Bebkirane et al. [15] works on an analytical and experimental study on contour machining based on neural network. This is more precise than the Taghuchi method for finding MRR. Singh R & Kamba J S [16] works on the density concepts of metal removal rate in ultrasonic machining. Also B.C. Routara et al. [17] work on the same concepts using Grey relationship analysis. Zhang et al. [18] works on ultrasonic assisted electrical discharge machining in gas to improve its efficiency. Choi et al. [19] works on chemical assisted ultrasonic machining of glass. Gauri S K [20] optimizes the correlated multiple responses of ultrasonic machining. They used weighted principle component method & principal component analysis for the better optimization performance of MRR. Zarepour H. & Ye SH [21] work on predictive modeling of material removal modes in micro ultrasonic machining. This model enhances the surface quality as well as improves the MRR. Liu et al. [22] developed a cutting force model for ultrasonic machining of brittle materials. This model is the first cutting force model for rotary ultrasonic machining of brittle materials and is also helpful to predict cutting temperature, tool wear, and surface roughness in RUM.

Sashay et al. [23] proposed an analytical model applied Monte Carlo simulation based crystal ball analysis tool to two popular mathematical models of USM namely Miller's model and M.C. Shaw's model. Effects of input variables such as abrasive particle size, particle concentration, amplitude of vibration, tool radius and depth of cut on MRR were analyzed for both models. Simulation of Shaw's model indicated that MRR decreases with increase in grain size. However, literature available on experimental data contradicts this and suggests just the reverse. Miller's model predicts a steeper relationship between grain size and MRR. Taratynov O V et al. [24] proposed a mathematical model for determining the height of surface projection after ultrasonic machining. They presented a very complex

mathematical equation for determining the height surface projection using dynamic pulse method. Recently Qinjian Z. et al. [25] works on ultrasonic assisted electrical discharge machining of polycrystalline diamond.

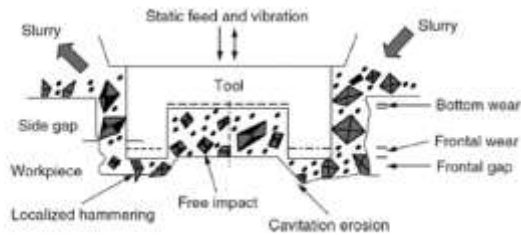


**Figure 1** USM material Mechanism

From all these models, four different mechanisms can be identified, which are responsible for removal of material from the work surface (Figure1). These are described as:

1. Material abrasion by direct hammering of the abrasive particles against the work piece surface.
2. Micro-chipping by impact of free moving particles.
3. Cavitation effect from the abrasive slurry.
4. Chemical action associated with the fluid employed.

The individual or combined effect of the above listed mechanisms results in material removal by shear or by fracture and by displacement of the material at surface, without removal, by plastic deformation, which occurred simultaneously at the transient surface. With porous materials such as graphite, cavitation erosion has been found to be a significant contributor of material removal as opposed to hardened steels and ceramics [26], Riddei, Bullet [27] and Willard [28] reported that the cavitation bubbles formed during the ultrasonic oscillations produce a pressure more than 1000 gf/cm<sup>2</sup> on the work surface when they collapse. This pressure rise also causes material removal. It has been reported that as long as the working gap between the tool and work piece surface is more than the mean size of the

abrasive grains used, no significant machining can take place [7].

The free impact mechanism has been found to be more effective and significant with larger grain sizes of abrasive used. With fine grit sizes of abrasive grains, the direct hammering mode has been found to be predominant for material removal. The initiation and propagation of median as well as lateral cracks has been considered to contribute greatly to the material removal process in ultrasonic machining [29] of ceramic composites. The sharp point of indenter (abrasive grain) produces an inelastic deformation zone and at some threshold, a deformation-induced flow suddenly develops into a small crack, termed as a median crack. An increase in the load causes further growth of the median crack. Figure 2 shows the mechanism of generation and propagation of cracks while machining ceramics in USM. During unloading, the median crack begins to close; inducing the formation of lateral vents [8]. Upon complete unloading, the lateral vents continue their extension towards the work surface and lead to chipping. Zarepour and Yeo [17] developed a model to predict ductile and brittle material removal modes while a brittle material is impacted by a single sharp abrasive particle in micro-ultrasonic machining process. The model was developed on the basis of indentation fracture theory. The quantitative criterion for brittle-ductile transition in material removal were evolved using threshold kinetic energy consideration; in promoting radial and lateral cracks. The outcome of this research could be used as a platform to build reliable models for prediction of MRR based on the material removal mode.

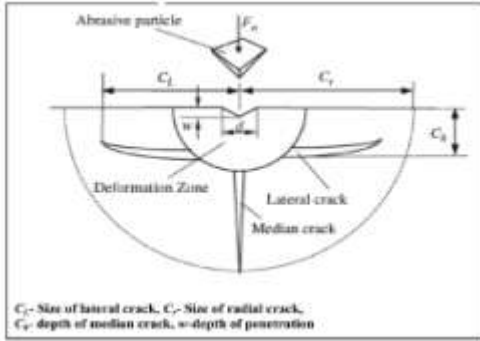


**Figure.2** Crack Propagation and work surface indentation in USM

considerations given to slurry circulation and abrasive selection, tolerances of the order of 1.00 cm can be achieved[30]. Holes of up to 64mm thickness can be drilled successfully without applying special efforts. Holes as small as 76 mm in Diameter can be drilled, however the depth to diameter ratio is limited to 3:1[29].When optimum flushing techniques are used, hole-depth capabilities can be extended to 150mm with aspect ratio up to 40:1 [31]. However, effective machining rate is reduced for machining of work piece thickness more than 12.7 mm, due to inefficient slurry flow through the cutting gap[32].Penetration rates, ranging from 0.025–25mm/min can be obtained depending upon the shape

## 2 MODEL DEVELOPMENT

In USM process, the mechanism of material removal can be described as the effect of the impact indentation and fracture phenomena. The impact indentation is a process in which a grit pushed by the end face of the tool head penetrates the work surface with a given speed. This impact is the combined effect of both the grits and the tool head, with their energy and momentum passing through the grits to the work. The impact indentation also causes crack initiation and development in the brittle work material beneath the contact area of each grit. The second phase is

called fracture. In this phase, cracks develop in an intermittent fashion with cyclic impacts, finally causing a layer of local work material beneath the grits to spall into tiny pieces in one of the later strikes. This cycle of impact indentation and fracture occurs repeatedly during the machining process. Other than this brittle failure of the work material due to indentation some material removal may occur due to free flowing impact of the abrasives against the work material and related solid-solid impact erosion, but it is estimated to be rather insignificant. Thus, in the current model, material removal would be assumed to take place only due to impact of abrasives between tool and work piece, followed by indentation and brittle fracture of the work piece. The model does consider the deformation of the contact zone.

The complete description of surface generated is very difficult due to the complex behavior of different grains because of the random grain-work interaction. Thus, certain assumptions have to be made while predicting the material removal rate. The assumptions are given as:

- (i) All the abrasive grains are considered to be identical in shape,
- (ii) An individual grain has many tiny cutting points on its surface (i.e. local spherical bulges), therefore, for simplicity, the grain tips are approximated as hemi spheres of diameter  $d_b$ , randomly distributed throughout the grain surface,
- (iii) The profile of the indentation generated is same,
- (iv) The average volume of material removed by impact indentation and fracture caused by each grain tip is considered to be a portion of a sphere ,
- (v) The maximum gap between the tool and the work allowable is about the same magnitude as the amplitude of vibration. In the current model, an

abrasive particle is considered to be spherical but with local spherical bulges as shown in Figure.3. The abrasive particles are characterized by the average grit diameter,  $d_g$ . It is further assumed that the local spherical bulges have a uniform diameter,  $d_b$  and which is related to the grit diameter by  $d_b = \mu d_g^2$ . Thus an abrasive is characterized by  $\mu$  and  $d_g$ .

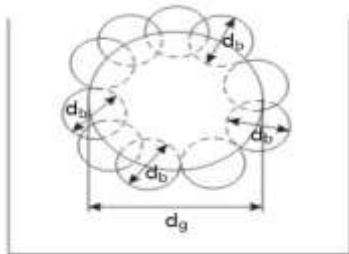


**Figure.3** Schematic representation of Abrasive Grit

During indentation by the abrasive grit onto the work piece and the tool, the local spherical bulges contact the surfaces and the indentation process is characterized by  $d_b$  rather than by  $d_g$ . Figure 4 (a) and (b) shows the interaction between the abrasive grit and the work piece and tool.

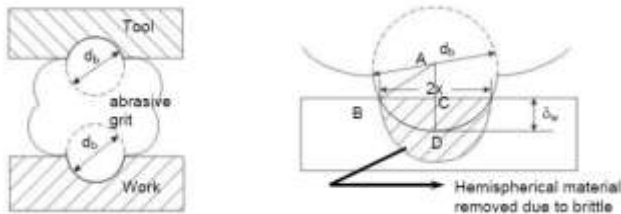


**Figure 4** (a) and (b) Interaction between grit and work piece and tool

As the indentation proceeds, the contact zone between the abrasive grit and work piece is established and the same grows. The contact zone is circular in nature and is characterized by its diameter ' $r_w$ '. At full indentation, the indentation depth in the work material is characterized by  $\delta_w$ . Due to the indentation, as the work material is brittle,

brittle fracture takes place leading to hemi-spherical fracture of diameter ' $r_w$ ' under the contact zone. As evident the machining rate is greatly affected by deflections that occur in the contact zone. The radius of the contact indentation zone is therefore an important determinant and depends on contact deflections which modify the shape of the contact zone. Geometrically, the contact deflections can influence both the material removal rate of the work piece and the accuracy of size of ground components. The contact deflection in ultrasonic machining can be viewed microscopically and macroscopically. Microscopically, the local spherical bulges of an abrasive grain are deflected by the static force exerted on it during machining and the work piece is deformed in the grinding zone. Macroscopically, the abrasive grit may be considered as a sphere pressed against a flat surface from which the material is to be removed. Due to elastic deformation, the grit-work piece contact zone radius and the deformed grit radius are increased. So the contact zone of deflections has two components, which are contributing to radius of the contact zone and that are

- a. The elastic deflection between the abrasive grit and the work piece.
- b. The microscopic contact at the local bulge level.

The real radius of the contact zone would be due to the combined effect of the two components. In order to calculate the real radius of the contact indentation zone, first of all, the mutual elastic deflection between the local spherical bulges of an abrasive grain and the work piece and the grit and the work piece are calculated from Hertz relations to get the real contact zone radius. Now the two modes of deflection (i.e. (a) and (b) as mentioned above) are separately considered. Firstly, the elastic deflection due to local spherical bulges of an abrasive grit-work piece contact, assuming that no elastic deflection of the grit takes place is considered. Secondly, the elastic deflection due to

the contact between the grit and the work piece, assuming the individual grit is undeformed is considered. These two modes are then combined to give the total contact deflection of the grain-work piece.

In order to calculate the elastic deflection of the local spherical bulges of an abrasive grain-work piece contact (assuming no elastic deflection of the grains), local spherical bulges, although irregular in shape, will be assumed spherical with diameter  $d_b$ . Considering a single local spherical bulge is pressed against a work piece surface under a normal load  $F_c$ ; the Hertz relations for a sphere [34] gives the mutual approach of remote points in the local spherical bulge and the work piece surface as

$$\delta_b = \sqrt[3]{(3\pi/2\sqrt{2})^2 (K_w + K_b)^2 (1/d_b) F_c^2} \quad (1)$$

Where  $F_c$  is the load applied to the grit,  $d_b$  is the mean diameter of the local spherical bulge. The work piece and grit elasticity can be estimated, respectively, by

$$K_i = (1 - \nu_i^2) / \pi E_i, \quad i = b(\text{local spherical bulge}), w(\text{workpiece})$$

Where  $E_i$  is the modulus of elasticity and  $\nu_i$  is the Poisson's ratio for the grit and work piece material. Similarly, in order to calculate the elastic deflection of the grain-workpiece contact, the elastic behavior of the grain can be approximated by assuming it to be continuum. It is reasonable for the present contact calculation; because the stresses will be compressive everywhere and the stressed region will be large, relative to the size of the local spherical bulges [33]. Assuming the machining to be continuum, the Hertz relations for contact between a spheres(i.e. grain) and a flat surface (i.e. work piece surface) can be applied. The radius of contact zone between grain and work piece surface will be given by[33] as;

$$r_g = \sqrt{2.56(\pi d_s / b)(K_w + K_g) F_c} \quad (2)$$

Where  $f_c$  the normal load and  $d_g$  is the diameter of the grain. The grain and work piece elasticity can be estimated, respectively by

$$K_i = (1 - \nu_i^2) / \pi E_i, \quad i = g(\text{grain}), w(\text{workpiece})$$

Where  $E_i$  is the modulus of elasticity and  $\nu_i$  is the Poisson's ratio for the grain and work piece material. In order to assess the combined local elastic deflection, it would be essential to club local elastic deflection caused by both the modes (i.e. the modes (a) and (b) as mentioned above). For deflection condition, the number of local spherical bulges contacting the work piece will be  $N_d$ . Since the distribution of local spherical bulges on the grain is random, it will be reasonable to assume that all local spherical bulges are equally loaded by the normal force. The condition of a grain under load and can be visualized in two steps. First the grain alone deflects; this gives a contact zone radius,  $r_b$ . Following this, local spherical bulges and work piece deflect, which will cause the radius of contact zone to increase. Since the radius of the grain is large as compared to the radius of the contact zone, it will be a reasonable approximation that the total radius of contact zone will be given by the sum of the radius of contact zones from the two deflections i.e.

$$r'_w \cong r_b + r_g \quad (3)$$

where  $r_g$  and  $r_b$  are the radiuses of contact zones as indicated in Figure.3.2 (a) and 2 (b), where  $r_g$  is given by Eq.(2), the radius of contact zone  $r_b$  is,  $r_b \cong 2\sqrt{d_b \delta_b}$  where  $\delta_b$  is the mutual approach of remote points in the local spherical bulges and the work piece, given by Eq. (3.1). The total radius of the contact zone  $r'_w$  can be evaluated by substituting the value of  $r_g$  and  $r_b$  in the Eq. (3). Substituting the value of  $r_g$  and  $r_b$  from Eq. (3) and,

in Eq. (4), the value of real radius of the contact zone  $r'_w$  can be expressed as

$$r'_w = 2\sqrt{\Phi d_b F_n^{1/3} + \Psi F_n^{1/2}}$$

Where,  $\Phi = \sqrt[3]{(3\pi/2\sqrt{2})^2 (K_w + K_b)^2 (1/d_g)}$  and  $\Psi = \sqrt{2.56(\pi d_s/b)(K_w + K_g)}$ . (4)

If the elastic properties  $K_w$ ,  $K_b$  and  $K_g$  are known, then Eq. (6) can be evaluated numerically to give the  $r'_w$  for a particular grain and work combination at any force,  $F_n$ . Similarly the total deflection ( $\delta$ ) would be the sum of two deflections i.e.  $\delta_g$  and  $\delta_b$  as given  $\delta = \delta_b + \delta_g$ . The actual depth of indentation of abrasive grain in the work piece after incorporating the contact deflection can be expressed as  $\delta'_w = \delta_w - \delta$ . Where  $\delta_w$  is the depth of indentation without considering the deflection caused due to grain-work piece interaction [34] and given by

$$\delta_w = \frac{d_g - y}{1 + q}$$
 (5)

Where,  $d_g$  is the average size of the abrasive grain,  $y$  is the distance between tool and work piece,  $q$  is the ratio of work piece hardness to tool hardness.

The volume  $V_g$  fracture per grit is given by the hemispherical portion [35], shown shaded in figure 2:

$$V_o = \frac{2}{3} \pi r_w'^3$$
 (6)

The material removal rate due to all the abrasive grains of diameter  $d_g$  is written in terms of the volume removed per grit; the number of abrasive particles of that diameter in the working gap and the frequency  $f_r$ :  $M_R = V_o \chi_d f_r$ . Where  $\chi_d$  gives the number of particles of size  $d$ . Since the maximum gap between the tool and the work allowable in USM is about the same magnitude as the amplitude of

vibration, it results in a limitation in the size of the grits that can participate in the machining. When the average grit size approaches the dimension of the gap, some of them with larger diameters will exceed the size of the gap and hence cannot get into the cutting zone to participate in the machining process, which reduces the number of active abrasive particles in action. Assuming  $\bar{d}$  to be the mean size of the grits in the working gap, the size distribution can be described as [36]:

$$\chi_d = 1.095 \frac{N}{\bar{d}} \left( 1 - \left( \frac{d}{\bar{d}} - 1 \right)^2 \right)^3$$

Where,  $\bar{d}$  is the mean diameter of the particles in the working gap and  $N$  is the number of particles in the working gap. The number of particles  $N$  is found from the weight of abrasive particles in the slurry. The volume of the working gap containing the abrasive slurry is

$$v_g = \frac{\pi}{4} D^2 y_t$$
 (7)

Where  $D$  is the tool diameter and  $y_t$  is the distance between the work piece and the tool at any instant of time  $t$ . If  $C$  is the concentration of abrasive particles in the slurry by weight, ( $C$  kg of abrasive in 1 kg of liquid) is the density of abrasive and  $\rho_a$  is the density of the liquid used for the abrasive slurry, and then the weight of the abrasive particles in the working gap at any instant of time will be

$$W_t = \frac{\pi D^2 C y_t}{4 \left( \frac{1}{\rho_f} + \frac{c}{\rho_a} \right)}$$
 (8)

The number of particles in the working gap at any instant of time  $t$  is:

$$N_t = \frac{W_t}{W}$$
 (9)

Where  $W$  is average weight of abrasive particles. The weight of an abrasive particle of diameter  $d$  is:

$$W_d = \frac{\pi}{6} d^3 \rho_a$$

Hence the average weight of particles in

$$W = \int_{d_0}^{d_m} (\pi/6) d^3 \rho_a \frac{\chi_d}{N} dd$$

the slurry is: Where  $d$  is the minimum diameter of the abrasive particles and  $d_m$  is the maximum diameter of the abrasive particles.

$$W = \left( \frac{0.57 \rho_a}{\bar{d}} \right) \int_{d_0}^{d_m} d^3 \left( 1 - \left( \frac{d}{\bar{d}} - 1 \right)^2 \right)^3 dd \tag{10}$$

Substituting the values of  $W_t$  and  $W$  in equation (9)

$$N_t = \frac{\pi D^2 c \bar{d}}{2.28 \left( \frac{\rho_a}{\rho_f} + c \right)} \left( \frac{y_t}{\int_{d_0}^{d_m} d^3 \left( 1 - \left( \frac{d}{\bar{d}} - 1 \right)^2 \right)^3 dd} \right) \tag{11}$$

The working gap  $y_t$  is given by (figure.3)

$$y_t = (x + y_0) - y_0 \sin \theta \tag{12}$$

The average working gap during the period between the instant when the tool touches the largest abrasive grain and the time when it stops at a distance  $y$  from the work piece is

$$\bar{y} = \frac{1}{\left( \frac{\pi}{2} - \theta_s \right)} \int_{\theta_s}^{\pi/2} ((y + y_0) - y_0 \sin \theta) d\theta$$

Where

$$\bar{y} = (x + y_0) - \left( y_0 \cos \theta_s / \left( \frac{\pi}{2} - \theta_s \right) \right) \tag{13}$$

$$\theta_s = \sin^{-1} y_s / y_0 \text{ And } y_s = y_0 - d_m + y$$

Hence, the average number of particles in the working gap is given by

$$N = \frac{\pi D^2 c \bar{d}}{2.28 \left( \frac{\rho_a}{\rho_f} + c \right)} \left( \frac{\bar{y}}{\int_{d_0}^{d_m} d^3 \left( 1 - \left( \frac{d}{\bar{d}} - 1 \right)^2 \right)^3 dd} \right) \tag{14}$$

The active grains taking part in material removal process are those having diameters between  $y$  (the distance between the tool and the work piece) and  $d_m$  (the maximum diameter of the abrasive grains).

The distance  $y$  of the tool from the work piece can be determined by equating the impulse due to the static force  $F_s$  over the entire cycle, to the impulse due to the variable contact force  $F_c$  acting over the contact portion of the cycle [36].

The impulse due to the static force  $F_s$  during the entire cycle is given as:

$$M_s = \frac{2\pi}{\omega} F_s \tag{15}$$

The contact force at a time  $t$  is

$$F_{ct} = \int_{y_{xt}}^{d_m} \pi d H_w \delta'_{wt} \chi_d dd \tag{16}$$

Where  $\delta'_{wt}$  is the indentation in the work piece at a time  $t$  for a particle of size  $d$  and is given by

$$\delta'_{wt} = \delta_{wt} - \delta_t$$

And  $\delta_{wt} = (d - y_t) / (1 + q)$  (17)

Hence, the contact force is given as:



$$F_{ct} = \int_{y_i}^{d_m} \pi H_w (\delta_{wt} - \delta_t) \chi_d d \tag{18}$$

The impulse due to the contact force during the contact period from  $\theta_s$  to  $\pi/2$  is

$$M_{ct} = \frac{1.095\pi NH_w}{d\omega} \int_{\theta_0}^{\pi/2} \int_{y_i}^{d_m} (\delta_{wt} - \delta_t) \left(1 - \left(\frac{d}{d} - 1\right)^2\right)^3 dd \cdot d\theta \tag{19}$$

Equating the static force impulse  $M_s$  to the contact force impulse  $M_{ct}$ , we get

$$\frac{2\pi F_s}{\omega} = \frac{1.095\pi NH_w}{d\omega} \int_{\theta_0}^{\pi/2} \int_{y_i}^{d_m} (\delta_{wt} - \delta_t) \left(1 - \left(\frac{d}{d} - 1\right)^2\right)^3 dd \cdot d\theta \tag{20}$$

Substituting for  $y_i$  from eq. (12), the integral in eq. (20) can be solved to give an expression in terms of  $y$ ,  $d_m$  and  $d$ . Equations (14) and (20) can then be solved for  $N$  and  $y$  to calculate the machining rate from eq. (1). Hence, the total material removal rate  $M_R$ , considering all the effective particles, is:

$$M_R = \int_y^{d_m} \frac{2\pi}{3} (\delta'_w d)^{3/2} \left( 1.095 \frac{N}{d} \left(1 - \left(\frac{d}{d} - 1\right)^2\right)^3 f_r dd \right)$$

Substituting for  $\delta'$  from equation (5) we get

$$M_R = \frac{2.29Nf_r}{(1+q)^{3/2} d} \int_y^{d_m} ((d-y)d) \left(1 - \left(\frac{d}{d}\right)^2\right)^3 dd \tag{21}$$

To find out the metal removal rate from equation (21), the average number of particles  $N$  and the distance  $y$  needs to be determined.

### 3 Results and discussion

The theoretical analysis is applied to study the effect of static load, amplitude of tool vibration and the mean size of

abrasive particles. The machining rate is found out by solving equations (14) and (20) for  $N$  and  $x$  and substituting the values in equation (1). A computer program is developed to obtain theoretical results for machining glass with a mild steel tool of 12.7 mm diameter at a frequency of 25.5 kc/sec using 400 mesh boron carbide abrasive in water as slurry. The following material properties were used: hardness of glass -470 kg/mm<sup>2</sup>, hardness of mild steel tool-150 kg/mm<sup>2</sup>. Its Young's modulus  $E$  is 68.65 X 10<sup>3</sup> N/mm<sup>2</sup>; the Poisson's ratio  $\nu$  is 0.17; and the density  $p$  is 1.452 X 10<sup>18</sup> kg/mm<sup>3</sup>. The cutting parameters are selected from the range commonly used in the USM machining: grit radius  $R$  is 10  $\mu Sm$ ; vibration amplitude  $Y$  is 100  $\mu m$ ; and vibration frequency is 20 kHz; when they are acting as constants. When they are variables, the range for  $R$  is (5.0-180)  $\mu m$ ;  $Y$  is (10-100)  $\mu m$ .

#### 3.1 Effect of static load and amplitude of vibration

The machining rate is calculated for different values of static load and amplitude. The results are shown in Figure.5 and 6. The curves show that the machining rate increases with an increase in the static load and amplitude of tool vibration. Thus the analysis predicts an infinite increase rate (Figure.6) agrees qualitatively with the experimental results of Nepiras as reported by Rozenberg[36]. However,

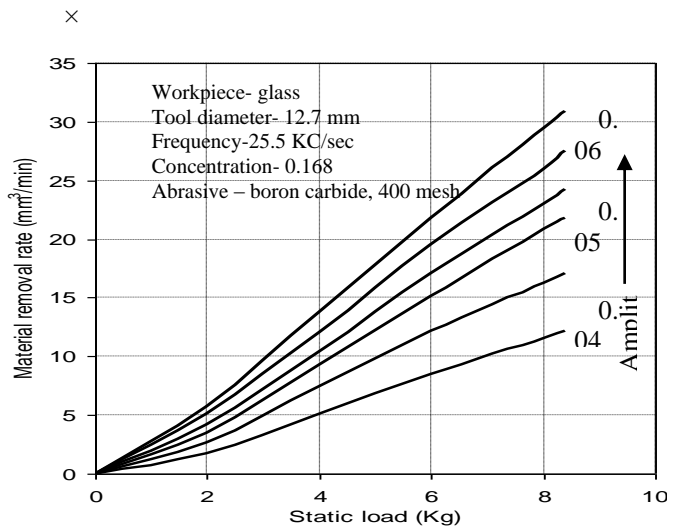


Figure.5 Variation of machining rate with static load.

an approximate comparison with experimental values quoted by Rozenberg[36] shows that the theoretical machining rate is an order higher than the practical value of about 32 mm<sup>3</sup>/min for soda glass. In machining rate with static load

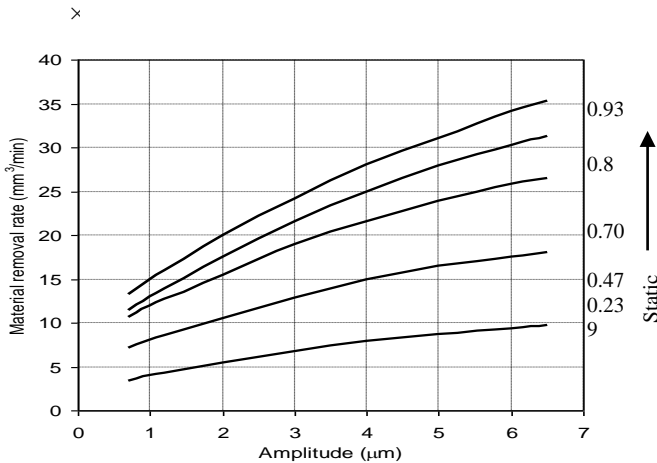


Figure 6 Variation of machining rate with amplitude.

However, in actual practice the machining rate first increases with static load and after reaching an optimum value, it falls with a further increase in static load [36]. The effect of amplitude on machining rate (Figure. 6) agrees qualitatively with the experimental results of Nepiras as reported by Rozenberg[36]. However, an approximate comparison with experimental values quoted by Rozenberg[36] shows that the theoretical machining rate is an order higher than the practical value of about 32 mm<sup>3</sup>/min for soda glass.

**3.2 Effect of size of abrasive grains**

The machining rate is calculated for various values of mean size of abrasive grains for amplitude of 0.0625 mm and a static load of 0.93 kg. The results plotted in Figure.7 predict a linear increase in machining rate with an increase in abrasive size whereas the experimental work of Fukumote

quoted by Rozenberg[36] shows an optimum value of grain size which depends upon the amplitude of the tool oscillation.

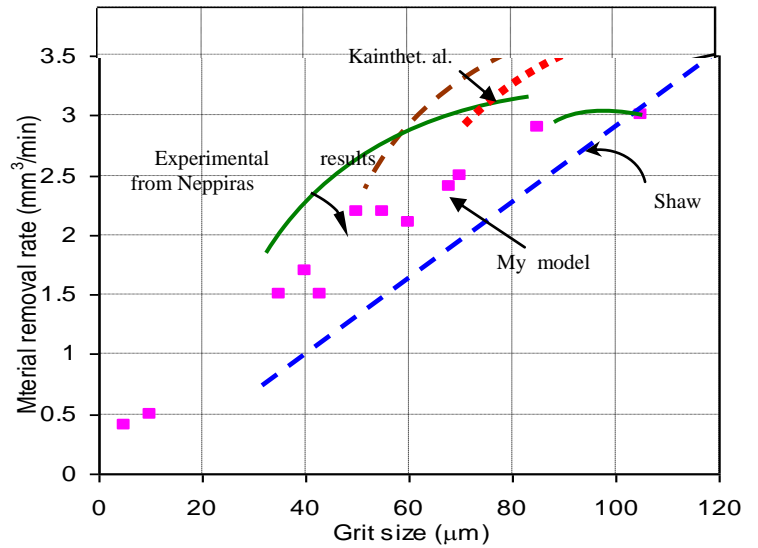


Figure 8 Comparison of theoretical and experimental results on MRR and grit size

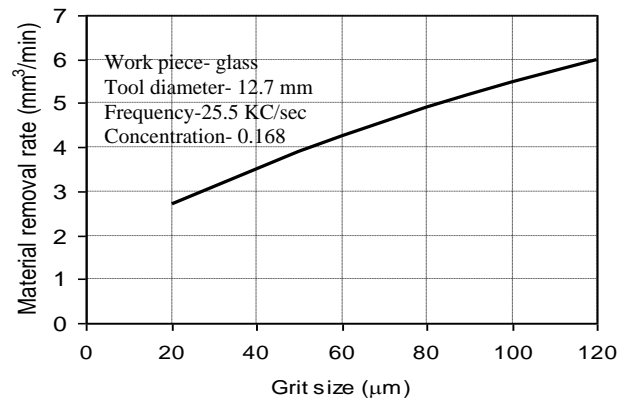


Figure 7 Estimated MRR and Grit size

**3.3 Comparison with the existing model**

From late 1960 onwards, considerable amount of experimental work has been carried out to study the effect of cutting parameters on the *MRR*. It is found that the *MRR* is linearly related to the grit size for smaller grits. However, when the average grit size becomes comparable with the amplitude (the gap) or beyond the amplitude (the gap), the

*MRR* decreases (Figure 7 solid line). This result has been confirmed by many investigations represented in the USM literatures. Some experiments confirmed only part of Neppiras' result because the many studies did not test the whole range of grit size [6].

The theoretical predictions from Shaw, Kainth et al. and the presented model are also plotted in dash lines in Figure 8. By comparing the three models with experimental results, it can be seen that the theoretical prediction presented in this paper is much closer to the practical results than the other two models.

#### 4 CONCLUSIONS

In this paper, a new analytical model for material removal rate prediction has been developed. The model incorporates the real deflection, which is in terms of the elastic properties of the tool and work piece material and the other traditional parameters. The elastic properties of the work piece material and the other parameters are also considered in the model. The proposed model results in a significant reduction in the depth of indentation, compared with that obtained by the existing model, under the same operating conditions. The elastic properties of both the tool and work piece cause a considerable deflection in the contact zone, resulting in an increase in the contact area of indentation and thereby decreasing the actual depth of indentation. This information gives a new understanding the depth of indentation in the contact zone, in terms of the elastic properties of the work and tool, has a strong influence on the material removal rate. In addition to this, the predicted *MRR*, based on this new model, shows a good agreement with experimental data obtained from different conditions, as compared to that calculated by the existing model, in machining glass. This information leads to an important conclusion that area of indentation can be controlled by properly controlling the different parameters. Hence, this model can be reliably used for the performance evaluation

of the ultrasonic machining process without conducting laborious experimentation.

#### REFENRENCE

- [1] Balamuth , L. A., Method of abrading, British Patent 602801,(1945)
- [2] Shaw, M. C., 1956, "Ultrasonic Grinding", *Microtechnic*, Vol. 10, No. 6, pp. 257-265.
- [3] G.E. Miller, Special theory of ultrasonic machining, *J. Appl. Phys.* 28 (1957) 149–156.
- [4] V. I.Dikushin and V N Barke ,” Ultrasonic Erosion and its dependence on the vibrational characteristics of the tool”, *Stonki I instrument*, No.5 , p.10 (1958)
- [5] L.D. Rosenberg, V.F. Kazantsev, L.O. Makarov, D.F. Yakhimovich, *Ultrasonic Cutting*, Consultant Bureau, New York, 1964
- [6] N.H. Cook, *Manufacturing Analysis*, Addison-Wesley, Reading, MA, 1966
- [7] Kainth G.S.et al. ,On the mechanics of material removal in ultrasonic machining, *International journal machine tool design research*, Vol 19,(1979)page 33-41
- [8] E.V. Nair, A. Ghosh, A fundamental approach to the study of the mechanics of ultrasonic machining, *Int. J. Prod. Res.* 23 (1985) 731–753.
- [9]Pei Z.J.,Prabhakar, D. ,Ferreira, P. M. , A mechanics approach to the prediction of material removal rates in rotary ultrasonic machining”, *manufacturing science & engineering*, ASME(1993) PED-Vol.64
- [10] H. Kamoun et al., Modeling the material removal in stationary mode for ultrasonic contour machining, in: *ASME Winter Annual Meeting*, 1993, pp. 759–770.
- [11]Wang Z Y &Rajurkar K P,Dynamic analysis of the ultrasonic machining process,*Journal of manufacturing science & engineering*,(1996)Vol.118.
- [12] Lee T C & Chan C W, Mechanism of the ultrasonic machining of ceramic composites, *Journal of machine processing technology* (1997), Vol: 71,195-201.
- [13] Wiercigroch, M.; Neilson, R.D.; Player, M.A. , Material removal rate prediction for ultrasonic drilling of hard materials using an impact oscillator approach. *Physics Letters*, 259:(1999) 91–96.
- [14] Yan Cherng Lin, BiingHwa Yan, Yong Song Chang,Machining characteristics of titanium alloy (Ti±6Al±4V) using a combination process of EDM with USM, *Journal of Materials Processing Technology* 104 (2000) 171-177.
- [15] Y. Benkirane, D. Kremer, A. Moisan,Ultrasonic Machining: an Analytical and Experimental Study on Contour Machining Based on Neural Network,Laboratories Proceeds Conventional ET Non-Conventional, ENSAM, Paris, France, and January (1998).

- [16] JS Kamba, Rupinder Singh, 2005, ultrasonic machining of titanium & its alloy, *Journal of machine processing technology*, 173(2006).
- [17] B.C. Routara, A.K. Sahoo, A.K. Rout and D.N. Thatoi, Optimization of multiple performance characteristics in ultrasonic machining process using Grey Relation Analysis, *Proceeding in International Conference on Mechanical Engineering* (2011).
- [18] Q H Zhang, R .Du. ,J H Zhang & Q B Zang,Ultrasonic assisted electrical discharge machining in gas, *International Journal of Machine Tools & Manufacture* 46 (2006) 1582–1588.
- [19] J.P. Choi , B.H. Jeon , B.H. Kim, Chemical-assisted ultrasonic machining of glass, *Journal of Materials Processing Technology* 191 (2007) 153–156.
- [20] Susanta Kumar Gauri, RinaChakravorty, Shankar Chakra borty, Optimization of correlated multiple responses of ultrasonic machining (USM) process, *International journal advance manufacturing technology*(2011), Vol: 53:1115-1127.
- [21]H.Zarepour, S.H. Yeo, Predictive modeling of material removal modes in micro ultrasonic machining, *International Journal of Machine Tools & Manufacture* 62 (2012) 13–23.
- [22] De Fu Liu , W.L. Cong , Z.J. Pei ,Yong Jun Tang, A cutting force model for rotary ultrasonic machining of brittle materials, *International Journal of Machine Tools & Manufacture* 52 (2012) 77–84.
- [23] Chittaranjan Sashay, SuhashGhosh, HariKiranKammila, An analysis of Ultrasonic machining using Monte Carlo simulation, *Proceeding of the ASME 2011International Mechanical Congress & Exposition*, November 11-17,2011,Denver ,Colorado,USA
- [24] O.V. Taratynov,V. V. Poroshin, and V.V.Kharchenko, Determining the height of surface projection after ultrasonic machining, *Russian Engineering Research*, Vol. 33, (2013), No. 1, pp. 53–56.
- [25] Z. Qinjian, Z. Luming, L. Jianyong, C. Yonglin, W. Heng, C. Yunan, S. Haikuo, Y.Xiaoqing, L. Minzhi, Study on electrical Discharge & ultrasonic assisted mechanical combine machining of polycrystalline diamond, *CIRP*, Vol.6.(2013)page no. 589-593.
- [26] Willard, G.W., Ultrasonically induced cavitation, *Journal of Acoustic Society of America*, 25: (1953) 669.
- [27] Ghahramani, B.; Wang, Z.Y., Precision ultrasonic machining process: A case study of stress analysis of ceramic (Al<sub>2</sub>O<sub>3</sub>), *International Journal of Machine Tools and Manufacture*, 41(8): (2001) 1189–1208
- [28]Tsutsumi, C.; Okano, K.; Suto, T., High quality machining of ceramics, *Journal of of Materials Processing Technology*, 37: (1993), 639–650.
- [29] Thoe, T.B.; Aspinwal , Review on ultrasonic machining, *International Journal of Machine Tools Manufacture*, 38(4): (1998), 239–255.
- [30] Kennedy, D.C.; Grieve R.J., Ultrasonic machining—A review, *The Production Engineer*, 54(9): (1975) 481–486.
- [31] Ghabrial, S.R. , Trends towards improving the surfaces produced by modern processes, *Wear*, 109(1–4): (1986), 113–118.
- [32] Barash, M.M.; Watanapongse, D.,On the effect of ambient pressure on the rate of material removal in ultrasonic machining, *International Journal of Mechanical Sciences*, 12: (1970), 775–779.
- [33] R.H. Brown, K. Saito, M.C. Shaw, Local Elastic Deflections in Grinding,*AnnalsoftheCIRP*19(1)(1971)105-113.
- [34] Komaraiah, M., Manan, M.A., Narsimha Reddy, and Victor, S., Investigation of surface roughness and accuracy in ultrasonic machining, *Precision engineering*, Vol.10, No.2, (1986), pp.59-65.
- [35] Guzzo PL, Shinohara AH), A comparative study on ultrasonic machining of hard and brittle materials, *J BrazSoc MechSciEng*26(1)(2004):56–64.
- [36] Rozenberg, L.D.; Kazantsev, V.F.; Makarov, L.O.,*Ultrasonic Cutting*, Consultant Bureau, New York, (1964) 97–102.
- [37] Neppiras, E.A., and Fosket, R.D., *Ultraschall-Materialbearbeitung*, Philips' Tech. Rundschau, Vol. 19(1957), pp. 37-39.